



Introducing Müntz-Kajani wavelet and its application in the numerical solution of a HIV infection of CD4⁺T cells model

Afkar Kareem Mnahi¹, Majid Tavassoli Kajani^{1,*}, Mohammed Jasim Mohammed², and Masoud Allame¹

¹Department of Mathematics, Isf. C., Islamic Azad University, Isfahan, Iran.

²Department of Mathematics, University of Thi-Qar, Nasiriyah, 64001, Iraq.

Abstract

In this paper, for the first time, we introduce a new wavelet called the Müntz-Kajani wavelet. We also study how to approximate a function by using these wavelets and provide an error bound. Then we use the collocation method based on the Müntz-Kajani wavelet to numerically solve a system of fractional differential equations. The accuracy of the solution is also assessed. To show how well the method works in practice, we apply it to investigate how HIV infects CD4⁺T cells. Numerical results are also given to demonstrate the efficiency and Cauchy convergence of the proposed method.

Keywords. Müntz -Kajani Wavelet, Fractional Differential Equations, Collocation Method, Approximation of the solution, Model of infected CD4⁺T cells by HIV.

2010 Mathematics Subject Classification. 65T60, 65Z05, 34A08.

1. INTRODUCTION

During the past decade, fractional calculus has been helpful in mathematical models in many different practical fields. Therefore, many scientists are interested in applying fractional calculus across various fields (see e.g. Gokmen et al. [15], Saffarian & Mohebbi [31], Canuto et al. [8], Maleki & Tavassoli Kajani [22], Tavassoli Kajani [33], Shirani et al. [32], Li et al. [19], Yang [37], Erman et al. [10], Liu & Jia [21], Celik et al. [9], Goel et al. [14]). Due to complexity in analytically solving fractional differential equations (FDEs), scientists who study applied mathematics are mainly interested in utilizing numerical methods for solving fractional order problems. In (Tural-Polat & Dincel [34]), multi-term variable-order fractional differential equations have been solved using shifted Chebyshev polynomials of the third kind. A hybrid function approach has been presented in (Postavaru & Toma [27]) for the numerical solution of two-dimensional fractional partial differential equations. In (Gande & Madduri [11]), fractional delay differential equations are solved via higher-order numerical schemes. Building on these developments, recent research efforts have introduced new techniques for solving fractional problems with increased efficiency. For example, in (Azodi & Yaghouti [5]), a method utilizing fourth-kind Chebyshev wavelets is proposed for solving a fractional-order HIV infection model involving Caputo derivatives. This approach approximates solutions as truncated series of wavelets, constructing an operational matrix of fractional integration to transform the problem into a nonlinear algebraic system. Similarly, (Amin et al. [4]) developed a Haar wavelet collocation method for HIV models, emphasizing error reduction and ease of implementation, with results compared to existing methods. Moreover, (Vivek et al. [35]) presents a Fibonacci wavelet-based algorithm that efficiently handles nonlinear differential equations associated with HIV models, providing accurate numerical results and graphical analysis. Furthermore, alternative numerical methods are proposed in (Roohollahi et al. [29], Babaei et al. [6], Irandoust-pakchin et al. [16], Ye et al. [38], Lemnaouar & Hattaf [20], Jain et al. [17], Katani et al. [18]) for solving fractional differential equations.

Received: 08 April 2025 ; Accepted: 16 August 2025.

* Corresponding author. Email: mtavassoli@iau.ac.ir .

Müntz functions possess unique attributes that make them applicable in different areas of mathematics, notably in the field of applied mathematics. Solving differential equations through numerical methods can be greatly facilitated by utilizing Müntz functions. They are particularly helpful in solving differential equations. In (Milovanović [25]), the author introduces Müntz orthogonal polynomials and discusses their numerical evaluation. In (Gandomani & Tavassoli Kajani [12]), the application of Müntz-Legendre Polynomials in solving a fractional order model of HIV Infection of CD4⁺T Cells is presented. Other studies about Müntz functions that show their additional applications can be found in the references (Aghashahi & Gandomani [1], Pourbabaee & Saadatmandi [28], Gandomani & Tavassoli Kajani [13], Marzban [23], Akhlaghi et al. [2, 3], Xu et al. [36], Sadek et al. [30]).

Here, is a brief explanation of what has been done in this article. In section 2, we briefly explain the initial concepts of fractional calculus. We also talk about Müntz functions and a type of wavelet called Müntz-Kajani wavelet for the first time. Furthermore, we study a new way to approximate a function using the Müntz-Kajani wavelet. In section 3, we derive a collocation method based on the Müntz-Kajani wavelets for solving fractional differential equations. In section 4, we provide an error analysis of the method of section 3. Section 5 is devoted one practical example, namely the infection process of HIV in CD4⁺T cells, by applying the method elucidated in section 3. Finally, we provide a concise summary and some conclusions in section 6.

2. INITIAL DEFINITIONS

2.1. Derivative and fractional integral.

Definition 2.1. Riemann Liouville fractional integral operator for the function $g \in L^2[0, 1]$ for $\sigma \in \mathbb{R}^+$ is defined as follows:

$$\mathcal{I}^\sigma g(x) = \frac{1}{\Gamma(\sigma)} \int_0^x \frac{g(s)}{(x-s)^{1-\sigma}} ds. \quad (2.1)$$

Definition 2.2. Caputo fractional derivative operator for the function $g \in L^2[0, 1]$ for $m-1 < \sigma \leq m$ is defined as follows:

$$\mathcal{D}^\sigma g(x) = \frac{1}{\Gamma(m-\sigma)} \int_0^x \frac{g^{(m)}(s)}{(x-s)^{\sigma+1-m}} ds. \quad (2.2)$$

According to the above definitions, for $\sigma \in \mathbb{R}^+$ and $m \in \mathbb{N}$, we have

$$\mathcal{I}^\sigma (\mathcal{D}^\sigma g(x)) = g(x) - \sum_{k=0}^{m-1} \frac{g^{(k)}(0)}{k!} x^k, \quad (2.3)$$

$$\mathcal{D}^\sigma g(x) = \mathcal{I}^{m-\sigma} (\mathcal{D}^m g(x)), \quad m-1 < \sigma \leq m. \quad (2.4)$$

2.2. Müntz orthogonal functions and their properties.

Definition 2.3. Family $\{\rho_m(x)\}_{m=0}^\infty$ expresses a class of orthogonal Müntz functions, which are orthogonal on the interval $[0, 1]$ with respect to the weight function $w(x) = 1$. These Müntz functions are defined as follows (Milovanović [25]):

$$\rho_m(x) = P_m(x) + \ln(x) Q_m(x), \quad x \in [0, 1], \quad m = 0, 1, 2, \dots \quad (2.5)$$

In which, $P_m(x)$ and $Q_m(x)$ are polynomials of order $\lfloor \frac{m}{2} \rfloor$ and $\lfloor \frac{m-1}{2} \rfloor$, respectively. Then we have

$$P_m(x) = \sum_{v=0}^{\lfloor \frac{m}{2} \rfloor} a_v^{(m)} x^v, \quad Q_m(x) = \sum_{v=0}^{\lfloor \frac{m-1}{2} \rfloor} b_v^{(m)} x^v. \quad (2.6)$$

If $m = 2n$, then for every $0 \leq v \leq n-1$, we have

$$a_v^{(2n)} = - \binom{n+v}{n}^2 \binom{n}{v}^2 \left(\frac{2n+1}{2v+1} + 2(n-v) \sum_{\substack{j=0 \\ j \neq v}}^{n-1} \frac{2j+1}{(j-v)(j+v+1)} \right), \quad (2.7)$$



and

$$b_v^{(2n)} = -(n-v) \binom{n+v}{n}^2 \binom{n}{v}^2, \tag{2.8}$$

and for $v = n$,

$$a_v^{(2n)} = \binom{2n}{n}^2, \quad b_v^{(2n)} = 0. \tag{2.9}$$

If $m = 2n + 1$, then for every $0 \leq v \leq n$, we have

$$a_v^{(2n)} = \binom{n+v}{n}^2 \binom{n}{v}^2 \left(\frac{2n+1}{2v+1} + 2(n+v+1) \sum_{\substack{j=0 \\ j \neq v}}^{n-1} \frac{2j+1}{(j-v)(j+v+1)} \right), \tag{2.10}$$

and

$$b_v^{(2n)} = (n+v+1) \binom{n+v}{n}^2 \binom{n}{v}^2. \tag{2.11}$$

Based on the definition 3, Müntz orthogonal functions can be identified using the following approach

$$\begin{aligned} \rho_0(x) &= 1, \\ \rho_1(x) &= 1 + \ln(x), \\ \rho_2(x) &= -3 + 4x - \ln(x), \\ \rho_3(x) &= 9 - 8x + 2 \ln(x)(1 + 6x), \\ \rho_4(x) &= -11 - 24x + 36x^2 - 2 \ln(x)(1 + 18x), \\ &\vdots \end{aligned} \tag{2.12}$$

Theorem 2.4. *The Müntz function $\rho_m(x)$ on the interval $[0, 1]$ has exactly m distinct simple roots (Milovanović [25]).*

Theorem 2.5. *Müntz functions are orthogonal and satisfy the following relation (Milovanović [25]):*

$$\int_0^1 \rho_i(x) \rho_j(x) dx = \begin{cases} \delta_j, & i = j, \\ 0, & i \neq j. \end{cases} \tag{2.13}$$

in which

$$\delta_j = \begin{cases} \frac{1}{j+1}, & \text{if } j \text{ is even,} \\ \frac{1}{j}, & \text{if } j \text{ is odd.} \end{cases} \tag{2.14}$$

2.3. The Müntz-Kajani wavelet and its properties. Wavelet families are generally come from the expansion and transformation of a function known as the mother wavelet. Here, we first divide the interval $[0, 1]$ into 2^k subintervals where $k = 0, 1, 2, \dots$. Then the Müntz-Kajani wavelet is formed as a result of the ongoing expansion and transformation in each of these subintervals:

$$\varphi_{i,j}(x) = \begin{cases} \sqrt{\frac{2^k}{\delta_j}} \rho_j(2^k x - (i-1)), & \text{if } x \in \left[\frac{i-1}{2^k}, \frac{i}{2^k}\right], \\ 0, & \text{Otherwise,} \end{cases} \quad i = 1, 2, \dots, 2^k, \quad j = 0, 1, 2, \dots \tag{2.15}$$

As a result, Müntz-Kajani wavelet is an orthogonal basis and we have

$$\int_0^1 \varphi_{i,j}(x) \varphi_{k,l}(x) dx = \begin{cases} 1, & \text{if } i = k \text{ and } j = l, \\ 0, & \text{if } i \neq k \text{ or } j \neq l. \end{cases} \tag{2.16}$$



Theorem 2.6. Müntz-Kajani wavelet $\varphi_{i,j}(x)$ on the interval $[\frac{i-1}{2^k}, \frac{i}{2^k}]$ has exactly j distinct simple roots.

Proof. If we consider the change of variable $z = 2^k x - (i - 1)$, then we have

$$\frac{i-1}{2^k} \leq x \leq \frac{i}{2^k} \iff 0 \leq z \leq 1$$

and

$$\varphi_{i,j}(x) = \sqrt{\frac{2^k}{\delta_j}} \rho_j(z), \quad \text{where } z = 2^k x - (i - 1). \quad (2.17)$$

On the other hand, based on Theorem 2.4, $\rho_j(z)$ for $0 \leq z \leq 1$ has j exact simple roots. Therefore $\varphi_{i,j}(x)$, for $\frac{i-1}{2^k} \leq x \leq \frac{i}{2^k}$ has j exact simple roots. \square

Remark 2.7. If $z_s, s = 1, 2, \dots, j$ are the roots of $\rho_j(z)$, then the roots of $\varphi_{i,j}(x)$ are given by

$$x_{i,s} = \frac{z_s + i - 1}{2^k}, \quad s = 1, 2, \dots, j, \quad i = 1, 2, \dots, 2^k. \quad (2.18)$$

2.4. Function approximation using the Müntz-Kajani wavelet. Assume that $g \in L^2[0, 1]$ and k is a positive integer. In this case, we approximate the function $g \in L^2[0, 1]$ using Müntz-Kajani wavelet as

$$g(x) \simeq \sum_{i=1}^{2^k} \sum_{j=0}^{N-1} c_{i,j} \varphi_{i,j}(x). \quad (2.19)$$

Now, based on the relation (2.16), the unknown coefficients $c_{i,j}$ are determined through the following approach:

$$c_{i,j} = \int_{\frac{i-1}{2^k}}^{\frac{i}{2^k}} g(x) \varphi_{i,j}(x) dx, \quad i = 1, 2, \dots, 2^k, \quad j = 0, 1, 2, \dots, N - 1. \quad (2.20)$$

For assessing the error of the above approximation, we would require the following definition.

Definition 2.8. The Sebolov space of the integer order r is represented by $H^r(0, 1)$ and is defined as follows (Canuto et al. [8]):

$$H^r(0, 1) = \left\{ v \in \mathbb{C}([0, 1]) : \frac{d}{dx} v^{(r-1)} \in L^2(0, 1) \right\}. \quad (2.21)$$

The members of $H^r(0, 1)$ can be accurately approximated using functions that are infinitely differentiable on $[0, 1]$.

Theorem 2.9. Suppose that $g \in H^r(0, 1)$ and $g = \sum_{i=1}^{2^k} g|_{I_i}$ such that $I_i = [\frac{i-1}{2^k}, \frac{i}{2^k}]$, $i = 1, 2, \dots, 2^k$, and

$$\Phi_i = \text{Span}\{\varphi_{i,0}(x), \varphi_{i,1}(x), \dots, \varphi_{i,N-1}(x)\}, \quad i = 1, 2, \dots, 2^k.$$

If $\tilde{g}|_{I_i} = \sum_{j=0}^{N-1} c_j \varphi_{i,j}(x)$ is the best approximation of $g(x)|_{I_i}$, then \tilde{g} represents an approximation to the function g with an upper error bound as follows:

$$\|g - \tilde{g}\|_{L^2(0,1)} = c N^{-r} (2^k)^{-r} \|g^{(r)}\|_{L^2(0,1)}.$$

Proof. Suppose that $P_N g(x)|_{I_i}$ is the finite Legendre approximation of $g(x)|_{I_i}$. According to the inequality (5.4.12) in Canuto et al. [8], the truncation error $(g(x) - P_N g(x))|_{I_i}$ is estimated as follows:

$$\left\| (g(x) - P_N g(x))|_{I_i} \right\|_{L^2(I_i)}^2 \leq c N^{-2r} (2^k)^{-2r} \left\| g^{(r)} \right\|_{L^2(I_i)}^2.$$

Hence, $P_N g(x)|_{I_i}$ is the best polynomial approximation of $g(x)|_{I_i}$ with respect to the norm L^2 in (Canuto et al. [8]), and we obtain

$$\left\| g(x)|_{I_i} - \tilde{g}(x)|_{I_i} \right\|_{L^2(I_i)}^2 = \left\| g(x)|_{I_i} - P_{N+1} g(x)|_{I_i} \right\|_{L^2(I_i)}^2 \leq c N^{-2r} (2^k)^{-2r} \left\| g^{(r)} \right\|_{L^2(I_i)}^2. \quad (2.22)$$



Finally,

$$\|g(x) - \tilde{g}(x)\|_{L^2(0,1)}^2 = \sum_{i=1}^{2^k} \|g(x)|_{I_i} - \tilde{g}(x)|_{I_i}\|_{L^2(I_i)}^2 \leq c N^{-2r} (2^k)^{-2r} \|g^{(r)}\|_{L^2(0,1)}^2, \tag{2.23}$$

which completes the proof. □

3. NUMERICAL SOLUTION OF FDES USING MÜNTZ-KAJANI WAVELET

The aim of this section is to describe a procedure for solving FDEs with the aid of a numerical method based on Müntz-Kajani wavelet.

3.1. Description of the method. Consider the following system of non-linear FDEs:

$$\begin{cases} \mathcal{D}^{\sigma_1} g_1(x) = F_1(x, g_1(x), g_2(x), \dots, g_n(x)), \\ \quad \vdots \\ \mathcal{D}^{\sigma_n} g_n(x) = F_n(x, g_1(x), g_2(x), \dots, g_n(x)), \end{cases} \quad x \in [0, 1], \tag{3.1}$$

with the initial conditions

$$g_1(0) = y_1, \quad g_2(0) = y_2, \quad \dots, \quad g_n(0) = y_n, \tag{3.2}$$

where \mathcal{D}^{σ_l} , $l = 1, 2, 3, \dots, n$ represents Caputo's fractional derivative operator of order $0 < \sigma_l \leq 1$. For the questions of existence and uniqueness results to the problem (3.1) refer to Baleanu et al. [7].

We first divide the interval $[0, 1]$ into 2^k , $k = 0, 1, 2, \dots$ equidistant subintervals. Then we present an approximation to the left side of Eq. (3.1) using the Müntz-Kajani wavelet on the i -th subinterval. That means:

$$\begin{cases} \mathcal{D}^{\sigma_1} g_{i,1}(x) = \sum_{j=0}^{N-1} c_{i,j}^1 \varphi_{i,j}(x), \\ \quad \vdots \\ \mathcal{D}^{\sigma_n} g_{i,n}(x) = \sum_{j=0}^{N-1} c_{i,j}^n \varphi_{i,j}(x), \end{cases} \tag{3.3}$$

where $c_{i,j}^l$ are the unknown coefficients in the approximation of the function $\mathcal{D}^{\sigma_l} g_l$, $l = 1, 2, \dots, n$ on the i -th subinterval using Müntz-Kajani wavelet.

To obtain an approximation for the functions g_l , $l = 1, 2, \dots, n$ via the relations expressed above and properties of Riemann–Liouville integral and Capute derivative, we have:

$$\begin{cases} g_{i,1}(x) = \mathcal{I}^{\sigma_1} \left(\sum_{j=0}^{N-1} c_{i,j}^1 \varphi_{i,j}(x) \right) + y_{i,1}, \\ \quad \vdots \\ g_{i,n}(x) = \mathcal{I}^{\sigma_n} \left(\sum_{j=0}^{N-1} c_{i,j}^n \varphi_{i,j}(x) \right) + y_{i,n}, \end{cases} \tag{3.4}$$

where

$$y_{i,l} = \begin{cases} y_l, & i = 1, \\ g_{i-1,l} \left(\frac{i-1}{2^k} \right), & i > 1, \end{cases} \quad \text{for } i = 1, 2, \dots, 2^k, \quad l = 1, 2, \dots, n.$$



In this way, the FDEs in Eq.(3.1) in the i -th subinterval can be rewritten as follows:

$$\begin{cases} \sum_{j=0}^{N-1} c_{i,j}^1 \varphi_{i,j}(x) = F_1(x, g_{i,1}(x), \dots, g_{i,n}(x)), \\ \vdots \\ \sum_{j=0}^{N-1} c_{i,j}^n \varphi_{i,j}(x) = F_n(x, g_{i,1}(x), \dots, g_{i,n}(x)). \end{cases} \quad (3.5)$$

Now, we substitute the roots of $\varphi_{i,N}(x)$, denoted by $x_{i,N}$, into the system (3.5) to arrive at

$$\begin{cases} \sum_{j=0}^{N-1} c_{i,j}^1 \varphi_{i,j}(x_{i,N}) = F_1(x_{i,N}, g_{i,1}(x_{i,N}), \dots, g_{i,n}(x_{i,N})), \\ \vdots \\ \sum_{j=0}^{N-1} c_{i,j}^n \varphi_{i,j}(x_{i,N}) = F_n(x_{i,N}, g_{i,1}(x_{i,N}), \dots, g_{i,n}(x_{i,N})). \end{cases} \quad (3.6)$$

As a result, Eq. (3.6) creates a system of nN algebraic equations with nN unknown coefficients. By solving this system using one of the existing methods and obtaining unknown coefficients $c_{i,j}^l$, approximations of the functions g_l , $l = 1, 2, \dots, n$ on the i -th subinterval will be found.

Remark 3.1. We know that for $i = 1, 2, \dots, 2^k$, $j = 0, 1, \dots, N-1$, $l = 1, 2, \dots, n$ the number of unknown coefficients $c_{i,j}^l$, is equal to $nN2^k$. Normally, when we have this number of unknown coefficients we reach a set of algebraic equations with dimensions $nN2^k \times nN2^k$; however, in the proposed method we have a system of 2^k algebraic equations with the dimensions $nN \times nN$, which leads to fewer mathematical calculations.

3.2. Error assessment. For assessing the convergence of the proposed method, we provide an error criterion. To clarify this, suppose that

$$\begin{cases} e_1 = g_1(x)|_{I_i} - \tilde{g}_1(x)|_{I_i}, \\ \vdots \\ e_n = g_n(x)|_{I_i} - \tilde{g}_n(x)|_{I_i}, \end{cases} \quad (3.7)$$

are the calculation errors for $g_l(x)|_{I_i}$, $i = 1, 2, \dots, 2^k$, $l = 1, 2, \dots, n$. Then

$$\begin{cases} R_1(x)|_{I_i} = \mathcal{D}^{\sigma_1} g_1(x)|_{I_i} - F_1(x, g_1(x)|_{I_i}, g_2(x)|_{I_i}, \dots, g_n(x)|_{I_i}), \\ \vdots \\ R_n(x)|_{I_i} = \mathcal{D}^{\sigma_n} g_n(x)|_{I_i} - F_n(x, g_1(x)|_{I_i}, g_2(x)|_{I_i}, \dots, g_n(x)|_{I_i}) \end{cases} \quad (3.8)$$

and

$$\begin{cases} \tilde{R}_1(x)|_{I_i} = \mathcal{D}^{\sigma_1} \tilde{g}_1(x)|_{I_i} - F_1(x, \tilde{g}_1(x)|_{I_i}, \tilde{g}_2(x)|_{I_i}, \dots, \tilde{g}_n(x)|_{I_i}), \\ \vdots \\ \tilde{R}_n(x)|_{I_i} = \mathcal{D}^{\sigma_n} \tilde{g}_n(x)|_{I_i} - F_n(x, \tilde{g}_1(x)|_{I_i}, \tilde{g}_2(x)|_{I_i}, \dots, \tilde{g}_n(x)|_{I_i}) \end{cases} \quad (3.9)$$



Hence, by subtracting the two previous equations, we arrive at

$$\begin{cases} E_1(x)|_{I_i} = R_1(x)|_{I_i} - \tilde{R}_1(x)|_{I_i} = \mathcal{D}^{\sigma_1} e_1(x)|_{I_i} - F_1(x, e_1(x)|_{I_i}, e_2(x)|_{I_i}, \dots, e_n(x)|_{I_i}), \\ \vdots \\ E_n(x)|_{I_i} = R_n(x)|_{I_i} - \tilde{R}_n(x)|_{I_i} = \mathcal{D}^{\sigma_n} e_n(x)|_{I_i} - F_n(x, e_1(x)|_{I_i}, e_2(x)|_{I_i}, \dots, e_n(x)|_{I_i}) \end{cases} \quad (3.10)$$

Finally, solving the following system of FDEs yields the approximation error:

$$\begin{cases} \mathcal{D}^{\sigma_1} e_1(x) = F_1(x, e_1(x), e_2(x), \dots, e_n(x)), \\ \vdots \\ \mathcal{D}^{\sigma_n} e_n(x) = F_n(x, e_1(x), e_2(x), \dots, e_n(x)) \end{cases} \quad x \in \left[\frac{i-1}{2^k}, \frac{i}{2^k} \right], \quad i = 1, 2, \dots, 2^k. \quad (3.11)$$

4. NUMERICAL SOLUTION OF HIV INFECTION OF CD4⁺T CELLS

In this section, we will analyze the transmission of CD4⁺T cells infection using the fractional model presented in reference (Gandomani & Tavassoli Kajani [12]). Consider the following model:

$$\begin{cases} \mathcal{D}^{\sigma_1} T(x) = q - \eta T(x) + rT(x) \left(1 - \frac{T(x)+1}{T_{max}} \right) - kV(x)T(x), \\ \mathcal{D}^{\sigma_2} I(x) = kV(x)T(x) - \beta I(x), \\ \mathcal{D}^{\sigma_3} V(x) = \mu\beta I(x) - \gamma V(x), \end{cases} \quad T(0) = T_0, \quad I(0) = I_0, \quad V(0) = V_0. \quad (4.1)$$

where $0 \leq x \leq 1$, $0 < \sigma_1, \sigma_2, \sigma_3 \leq 1$. The interpretation of the unknown functions and parameters is provided in Table 1. According to (Ongun [26]) the parameters of the model are considered based on physical or medical

TABLE 1. List of unknown functions and parameters.

Unknown functions	Meaning
$T(x)$	The concentration of uninfected CD4 ⁺ T in the blood
$I(x)$	The concentration of infected CD4 ⁺ T in the blood
$V(x)$	The concentration of HIV virus particle in the blood
Parameters	Meaning
η	Turnover rate of uninfected CD4 ⁺ T cells
β	Turnover rate of infected CD4 ⁺ T cells
γ	Turnover rate of HIV virus particles
$1 - \frac{T(x)+1}{T_{max}}$	Logistic growth indicator of uninfected CD4 ⁺ T cells
k	The infection rate of CD4 ⁺ T cells by HIV virus
kVT	The incident of HIV infection of healthy CD4 ⁺ T
μ	The number of virus particles produced by each infected CD4 ⁺ T cells during its life time
q	The generation rate of uninfected CD4 ⁺ T cells in the body
$\mu\beta$	The generation rate of virions through infected CD4 ⁺ T cells
T_{max}	The maximal concentration of CD4 ⁺ T cells in the blood
r	The rate of cell duplication through mitosis when they are stimulated by antigens and mitogens

consideration that are given as follows:

$$\begin{aligned} T_0 = 0.1, \quad I_0 = 0, \quad V_0 = 0.1, \\ q = 0.1, \quad \eta = 0.02, \quad \beta = 0.3, \quad r = 3, \quad \gamma = 2.4, \\ k = 0.00027, \quad T_{max} = 1500, \quad \mu = 10. \end{aligned} \quad (4.2)$$



Here, we assume that $\sigma = \sigma_1 = \sigma_2 = \sigma_3$ and we solve it for $\sigma = 1, 0.75$ and 0.5 . Table 2, Table 4 and Table 6 respectively show the values obtained for $T(x)$, $I(x)$ and $V(x)$ for $N = 5, 10, 15$ and $k = 3, 4, 5, 6, 7$ when $\sigma = 1$. From these three tables, we observe that incrementing in N and k cause the obtained value to have Cauchy convergence. For instance, for a fixed N and two consecutive values of k we have the following error:

$$\begin{aligned} \left| T(x) \Big|_{k=7}^{N=15} - T(x) \Big|_{k=6}^{N=15} \right| &\leq 9 \times 10^{-27}, \\ \left| I(x) \Big|_{k=7}^{N=15} - I(x) \Big|_{k=6}^{N=15} \right| &\leq 9 \times 10^{-34}, \\ \left| V(x) \Big|_{k=7}^{N=15} - V(x) \Big|_{k=6}^{N=15} \right| &\leq 9 \times 10^{-28}. \end{aligned} \quad (4.3)$$

Furthermore, for a fixed k and two values for N we have

$$\begin{aligned} \left| T(x) \Big|_{k=7}^{N=15} - T(x) \Big|_{k=7}^{N=10} \right| &\leq 9 \times 10^{-19}, \\ \left| I(x) \Big|_{k=7}^{N=15} - I(x) \Big|_{k=7}^{N=10} \right| &\leq 9 \times 10^{-26}, \\ \left| V(x) \Big|_{k=7}^{N=15} - V(x) \Big|_{k=7}^{N=10} \right| &\leq 9 \times 10^{-21}. \end{aligned} \quad (4.4)$$

Tables 3, 5, and 7 respectively report the values of $T(x)$, $I(x)$ and $V(x)$ obtained using some other methods when $\sigma = 1$. Comparisons between Tables 2, 4, and 6 with Tables 3, 5, and 7 show that our numerical results are in agreement with other methods in the literature and our method is capable of providing more accurate results. Tables 8, 9, and 10 respectively give the values of $T(x)$, $I(x)$ and $V(x)$ obtained using the present method when $\sigma = 0.75$. Moreover, Tables 11, 12, and 13 respectively show the values of $T(x)$, $I(x)$ and $V(x)$ when $\sigma = 0.5$. As it is clear in these tables, we also have Cauchy convergence. Figure 1 shows the $T(x)$ diagram, Figure 2 shows the $I(x)$ diagram and Figure 3 shows the $V(x)$ diagram for $\sigma = 0.5, 0.75, 1$. From Figure 1 we observe that the concentration of uninfected CD4⁺T cells in the blood is increasing as the time increased. Moreover, Figure 2 shows that the concentration of infected CD4⁺T cells is remains almost unchanged. Furthermore, Figure 3 reveals that the concentration of HIV virus particles in the blood is decreased. Finally, we conclude from Figures 1–3 that our method has analyzed the transmission of CD4⁺T cells infection, correctly.

5. CONCLUSION

In this article, a spectral collocation method based on a class of Müntz wavelets, called Müntz-Kajani wavelets, has been proposed for solving systems of FDEs. The Müntz-Kajani wavelet was introduced for the first time and an upper bound for its approximation was derived. The error of the proposed method was also assessed. The efficiency and spectral accuracy of the method was demonstrated on an applied model describing the HIV infection of CD4⁺T cells. It was shown that by increasing N and k the accuracy can be improved. Moreover, comparisons with some existing methods in the literature show the superiority of our method. It is recommended that future studies continue to explore the areas that provide more comprehensive understanding of the topic.

Declaration of competing interest

The authors declare that they have no known competing financial interests or personal relationships that could have appeared to influence the work reported in this paper.

Data availability

The data that support the findings of this study are openly available through the text.



TABLE 2. The values of $T(x)$ for $\sigma = 1$ and different values of N and k and comparison with other methods.

x	$N = 5$					
	$k = 3$	$k = 4$	$k = 5$	$k = 6$	$k = 7$	$k = 7$
0	0.1	0.1	0.1	0.1	0.1	0.1
0.2	0.20873643040	0.20873707213	0.20873704699	0.20873704677998716224	0.20873704677998716266	0.20873704677998716266
0.4	0.40596435533	0.40596356440	0.40596355837	0.405963557208282510393	0.40596355720828251091	0.40596355720828251091
0.6	0.76363239335	0.76363188159	0.76363200607	0.76363200047723818878	0.76363200047723818246	0.76363200047723818246
0.8	1.41206431836	1.41206390582	1.41206383514	1.41206384729221672566851120	1.412063847292216725683	1.412063847292216725683
1	2.58698689387	2.58698665052	2.58698662119	2.58698661711737932386	2.58698661711737932386	2.58698661711737932386

x	$N = 10$					
	$k = 3$	$k = 4$	$k = 5$	$k = 6$	$k = 7$	$k = 7$
0	0.1	0.1	0.1	0.1	0.1	0.1
0.2	0.20873704677	0.20873707213	0.20873704699	0.20873704677998716224	0.20873704677998716266	0.20873704677998716266
0.4	0.40596355720	0.40596356440	0.40596355837	0.405963557208282510393	0.40596355720828251091	0.40596355720828251091
0.6	0.76363200047	0.76363188159	0.76363200607	0.76363200047723818878	0.76363200047723818246	0.76363200047723818246
0.8	1.41206384729	1.41206390582	1.41206383514	1.41206384729221672566851120	1.412063847292216725683	1.412063847292216725683
1	2.58698661711	2.58698665052	2.58698662119	2.58698661711737932386	2.58698661711737932386	2.58698661711737932386

x	$N = 15$					
	$k = 3$	$k = 4$	$k = 5$	$k = 6$	$k = 7$	$k = 7$
0	0.1	0.1	0.1	0.1	0.1	0.1
0.2	0.20873704677998716357	0.2087370467799871626861	0.2087370467799871626861	0.2087370467799871626861	0.2087370467799871626861	0.2087370467799871626861
0.4	0.405963557208282511111	0.4059635572082825110393	0.4059635572082825110393	0.4059635572082825110393	0.4059635572082825110393	0.4059635572082825110393
0.6	0.763632000477238182229	0.7636320004772381824866	0.7636320004772381824866	0.7636320004772381824866	0.7636320004772381824866	0.7636320004772381824866
0.8	1.41206384729221672698	1.4120638472922167256681	1.4120638472922167256681	1.41206384729221672566851120	1.41206384729221672566851120	1.41206384729221672566851120
1	2.58698661711737932394	2.5869866171173793239373	2.5869866171173793239373	2.58698661711737932393731127	2.586986617117379323937311228	2.586986617117379323937311227

TABLE 3. Numerical results of other methods for $T(x)$.

x	LADM-Pade [26]	Method in [39]	VIM [24]	Method in [12]
0	0.1	0.1	0.1	0.1
0.2	0.2088072731	0.2038616561	0.2088073214	0.208808084
0.4	0.4061052625	0.3803309335	0.4061346587	0.406240543
0.6	0.7611467713	0.6954623767	0.7624530350	0.766442390
0.8	1.3773198590	1.2759624442	1.3978805880	1.414046852
1	2.3291697610	2.3832277428	2.5067466690	2.591559480



TABLE 4. The values of $I(x)$ for $\sigma = 1$ and different values of N and k and comparison with other methods.

x	$N = 5$		$N = 10$		$N = 15$	
	$k = 3$	$k = 4$	$k = 5$	$k = 6$	$k = 7$	$k = 8$
0	0.1	0.1	0.1	0.1	0.1	0.1
0.2	6.03157063749 × 10 ⁻⁷	6.03157315594 × 10 ⁻⁷	6.03157301873 × 10 ⁻⁷	6.03157301409 × 10 ⁻⁷	6.03157301375 × 10 ⁻⁷	6.03157301375 × 10 ⁻⁷
0.4	1.31529055603 × 10 ⁻⁶	1.31529033788 × 10 ⁻⁶	1.31529032305 × 10 ⁻⁶	1.31529032247 × 10 ⁻⁶	1.31529032244 × 10 ⁻⁶	1.31529032244 × 10 ⁻⁶
0.6	2.12086469305 × 10 ⁻⁶	2.1208648794 × 10 ⁻⁶	2.12086489240 × 10 ⁻⁶	2.12086489050 × 10 ⁻⁶	2.12086489030 × 10 ⁻⁶	2.12086489030 × 10 ⁻⁶
0.8	3.01426874794 × 10 ⁻⁶	3.01426817118 × 10 ⁻⁶	3.01426815894 × 10 ⁻⁶	3.01426815637 × 10 ⁻⁶	3.01426815600 × 10 ⁻⁶	3.01426815600 × 10 ⁻⁶
1	3.99638203619 × 10 ⁻⁶	3.99638170624 × 10 ⁻⁶	3.99638166773 × 10 ⁻⁶	3.99638166298 × 10 ⁻⁶	3.99638166239 × 10 ⁻⁶	3.99638166239 × 10 ⁻⁶

x	$N = 15$		$N = 10$		$N = 15$	
	$k = 3$	$k = 4$	$k = 5$	$k = 6$	$k = 7$	$k = 8$
0	0	0	0	0	0	0
0.2	6.03157301376 × 10 ⁻⁷	6.03157315594 × 10 ⁻⁷	6.03157301873 × 10 ⁻⁷	6.03157301376451171 × 10 ⁻⁷	6.03157301376451171 × 10 ⁻⁷	6.03157301376451171 × 10 ⁻⁷
0.4	1.31529032242 × 10 ⁻⁶	1.31529033788 × 10 ⁻⁶	1.31529032305 × 10 ⁻⁶	1.31529032242875816 × 10 ⁻⁶	1.31529032242875816 × 10 ⁻⁶	1.31529032242875816 × 10 ⁻⁶
0.6	2.12086489027 × 10 ⁻⁶	2.12086489794 × 10 ⁻⁶	2.12086489240 × 10 ⁻⁶	2.1208648902777102 × 10 ⁻⁶	2.1208648902777102 × 10 ⁻⁶	2.1208648902777102 × 10 ⁻⁶
0.8	3.01426815595 × 10 ⁻⁶	3.01426817118 × 10 ⁻⁶	3.01426815894 × 10 ⁻⁶	3.0142681559557427 × 10 ⁻⁶	3.0142681559557427 × 10 ⁻⁶	3.0142681559557427 × 10 ⁻⁶
1	3.99638166231 × 10 ⁻⁶	3.99638170624 × 10 ⁻⁶	3.99638166773 × 10 ⁻⁶	3.99638166231441987 × 10 ⁻⁶	3.99638166231441987 × 10 ⁻⁶	3.99638166231441988 × 10 ⁻⁶

TABLE 5. Numerical results of other methods for $I(x)$.

x	$k = 3$		$k = 4$		$k = 5$		$k = 6$		$k = 7$	
	LADM-Pade [26]	Method in [39]	VIM [24]	Method in [12]	LADM-Pade [26]	Method in [39]	VIM [24]	Method in [12]	LADM-Pade [26]	Method in [39]
0	0	0	0	0	0	0	0	0	0	0
0.2	0.603270728 × 10 ⁻⁵	0.6247872100 × 10 ⁻⁵	0.6032634366 × 10 ⁻⁵	0.603270224 × 10 ⁻⁵	0.603270728 × 10 ⁻⁵	0.6247872100 × 10 ⁻⁵	0.6032634366 × 10 ⁻⁵	0.603270224 × 10 ⁻⁵	0.603270728 × 10 ⁻⁵	0.6247872100 × 10 ⁻⁵
0.4	0.131591617 × 10 ⁻⁴	0.1293552225 × 10 ⁻⁴	0.1314878543 × 10 ⁻⁴	0.131583409 × 10 ⁻⁴	0.131591617 × 10 ⁻⁴	0.1293552225 × 10 ⁻⁴	0.1314878543 × 10 ⁻⁴	0.131583409 × 10 ⁻⁴	0.131591617 × 10 ⁻⁴	0.1293552225 × 10 ⁻⁴
0.6	0.212683688 × 10 ⁻⁴	0.2035267183 × 10 ⁻⁴	0.2101417193 × 10 ⁻⁴	0.212237854 × 10 ⁻⁴	0.212683688 × 10 ⁻⁴	0.2035267183 × 10 ⁻⁴	0.2101417193 × 10 ⁻⁴	0.212237854 × 10 ⁻⁴	0.212683688 × 10 ⁻⁴	0.2035267183 × 10 ⁻⁴
0.8	0.300691867 × 10 ⁻⁴	0.2837302120 × 10 ⁻⁴	0.2795130456 × 10 ⁻⁴	0.301774201 × 10 ⁻⁴	0.300691867 × 10 ⁻⁴	0.2837302120 × 10 ⁻⁴	0.2795130456 × 10 ⁻⁴	0.301774201 × 10 ⁻⁴	0.300691867 × 10 ⁻⁴	0.2837302120 × 10 ⁻⁴
1	0.398736542 × 10 ⁻⁴	0.3690842367 × 10 ⁻⁴	0.2431562317 × 10 ⁻⁴	0.400378155 × 10 ⁻⁴	0.398736542 × 10 ⁻⁴	0.3690842367 × 10 ⁻⁴	0.2431562317 × 10 ⁻⁴	0.400378155 × 10 ⁻⁴	0.398736542 × 10 ⁻⁴	0.3690842367 × 10 ⁻⁴



TABLE 6. The values of $V(x)$ for $\sigma = 1$ and different values of N and k and comparison with other methods.

x	$N = 5$						
	$k = 3$	$k = 4$	$k = 5$	$k = 6$	$k = 7$	$k = 8$	$k = 9$
0	0.1	0.1	0.1	0.1	0.1	0.1	0.1
0.2	0.061878427179	0.061878491915	0.061878489583	0.061878489570	0.061878489564	0.061878489564	0.061878489564
0.4	0.038289870018	0.038289848508	0.038289848400	0.038289848345	0.038289848354	0.038289848354	0.038289848354
0.6	0.023693959713	0.023693951243	0.023693952707	0.023693952707	0.023693952706	0.023693952706	0.023693952706
0.8	0.014662662061	0.014662661716	0.014662661432	0.014662661432	0.014662661429	0.014662661429	0.014662661429
1	0.009074697047	0.009074696832	0.009074696797	0.009074696792	0.009074696791	0.009074696791	0.009074696791

x	$N = 10$						
	$k = 3$	$k = 4$	$k = 5$	$k = 6$	$k = 7$	$k = 8$	$k = 9$
0	0.1	0.1	0.1	0.1	0.1	0.1	0.1
0.2	0.0618784895	0.0618784919	0.061878489583	0.06187848956086104661	0.06187848956086104945	0.06187848956086104945	0.06187848956086104945
0.4	0.0382898483	0.0382898485	0.03828984800	0.0382898483544682457291	0.0382898483544682457291	0.0382898483544682457291	0.0382898483544682457291
0.6	0.0236939527	0.0236939512	0.023693952771	0.02369395270581996649568375303780	0.02369395270581996649568375303780	0.02369395270581996649568375303780	0.02369395270581996649568375303780
0.8	0.0146626614	0.0146626617	0.014662661376	0.0146626614290444608535361737619	0.0146626614290444608535361737619	0.0146626614290444608535361737619	0.0146626614290444608535361737619
1	0.0090746967	0.0090746968	0.009074696797	0.0090746967917549909577	0.0090746967917549909577	0.0090746967917549909577	0.0090746967917549909577

x	$N = 15$						
	$k = 3$	$k = 4$	$k = 5$	$k = 6$	$k = 7$	$k = 8$	$k = 9$
0	0.1	0.1	0.1	0.1	0.1	0.1	0.1
0.2	0.06187848956560861047321	0.06187848956560861049579680	0.0618784895656086104957985984	0.0618784895656086104957986530850	0.0618784895656086104957986530850	0.0618784895656086104957986530850	0.0618784895656086104957986530850
0.4	0.038289848355720828251111817	0.03828984835446824573203958	0.038289848354468245732055623	0.0382898483544682457320556474497	0.0382898483544682457320556474497	0.0382898483544682457320556474497	0.0382898483544682457320556474497
0.6	0.02369395270581996495681850	0.02369395270581996495681850	0.0236939527058199649568375303780	0.0236939527058199649568375303780	0.0236939527058199649568375303780	0.0236939527058199649568375303780	0.0236939527058199649568375303780
0.8	0.01466266142904446085353704	0.01466266142904446085353704	0.0146626614290444608535361494	0.0146626614290444608535361737619	0.0146626614290444608535361737619	0.0146626614290444608535361737619	0.0146626614290444608535361737619
1	0.00907469679175499095768023	0.00907469679175499095768023	0.0090746967917549909576802423	0.0090746967917549909576802424178	0.0090746967917549909576802424178	0.0090746967917549909576802424178	0.0090746967917549909576802424178

TABLE 7. Numerical results of other methods for $V(x)$.

x	LADM-Pade [26]	Method in [39]	VIM [24]	Method in [12]
0	0.1	0.1	0.1	0.1
0.2	0.06187996025	0.06187991856	0.06187995314	0.0618799843
0.4	0.03831324883	0.03829493490	0.03830820126	0.038294888
0.6	0.02439174349	0.02370431860	0.02392029257	0.023704530
0.8	0.009967218934	0.01467956982	0.01621704553	0.014680364
1	0.003305076447	0.02370431861	0.01608418711	0.0091008450



TABLE 8. The values of $T(x)$ for $\sigma = 0.75$, $k = 0$ and different values of N .

x	$N = 20$	$N = 25$	$N = 30$	$N = 35$	$N = 40$
0	0.1	0.1	0.1	0.1	0.1
0.2	0.36631120808	0.36631120542	0.36631120472	0.36631120467	0.36631120471
0.4	0.93954736276	0.93954736026	0.93954736065	0.93954736043	0.93954736049
0.6	2.27860766035	2.27860765808	2.27860765729	2.27860765727	2.27860765727
0.8	5.41508374662	5.41508374220	5.41508374131	5.41508374107	5.41508374099
1	12.7257732426	12.7257732326	12.7257732305	12.7257732300	12.7257732298

TABLE 9. The values of $I(x)$ for $\sigma = 0.75$, $k = 0$ and different values of N .

x	$N = 20$	$N = 25$	$N = 30$	$N = 35$	$N = 40$
0	0	0	0	0	0
0.2	$1.21260512316 \times 10^{-6}$	$1.21260509803 \times 10^{-6}$	$1.21260509224 \times 10^{-6}$	$1.21260509172 \times 10^{-6}$	$1.21260509196 \times 10^{-6}$
0.4	$2.81349739936 \times 10^{-6}$	$2.81349735251 \times 10^{-6}$	$2.81349736137 \times 10^{-6}$	$2.81349735859 \times 10^{-6}$	$2.81349735936 \times 10^{-6}$
0.6	$5.55568985877 \times 10^{-6}$	$5.55568979667 \times 10^{-6}$	$5.55568978942 \times 10^{-6}$	$5.55568979211 \times 10^{-6}$	$5.55568979209 \times 10^{-6}$
0.8	$1.06436609879 \times 10^{-5}$	$1.06436609017 \times 10^{-5}$	$1.06436608861 \times 10^{-5}$	$1.06436608827 \times 10^{-5}$	$1.06436608817 \times 10^{-5}$
1	$2.04996562275 \times 10^{-5}$	$2.04996561099 \times 10^{-5}$	$2.04996561221 \times 10^{-5}$	$2.04996561175 \times 10^{-5}$	$2.04996561182 \times 10^{-5}$

TABLE 10. The values of $V(x)$ for $\sigma = 0.75$, $k = 0$ and different values of N .

x	$N = 20$	$N = 25$	$N = 30$	$N = 35$	$N = 40$
0	0.1	0.1	0.1	0.1	0.1
0.2	0.04964395587431	0.04964395438810	0.04964395412478	0.04964395412668	0.04964395415120
0.4	0.03358508711303	0.03358508658159	0.03358508678163	0.03358508670414	0.03358508673608
0.6	0.02507808424676	0.02507808433558	0.02507808405278	0.02507808407747	0.02507808410013
0.8	0.01987974971786	0.01987975001080	0.01987975004004	0.01987975004074	0.01987975003886
1	0.01642206024850	0.01642206068064	0.01642206059268	0.01642206061520	0.01642206060771



TABLE 11. The values of $T(x)$ for $\sigma = 0.5$, $k = 0$ and different values of N .

x	$N = 20$	$N = 25$	$N = 30$	$N = 35$	$N = 40$
0	0.1	0.1	0.1	0.1	0.1
0.2	1.4926333632	1.4910896912	1.4910072974	1.4910097428	1.4910101323
0.4	9.0813284103	9.0801123972	9.0802196110	9.0802120008	9.0802124122
0.6	50.262189304	50.261309657	50.261133340	50.261139800	50.261140025
0.8	215.63006163	215.63092060	215.63093897	215.63093840	215.63093829
1	526.85599196	526.85860856	526.85852432	526.85852398	526.85852422

TABLE 12. The values of $I(x)$ for $\sigma = 0.5$, $k = 0$ and different values of N .

x	$N = 20$	$N = 25$	$N = 30$	$N = 35$	$N = 40$
0	0	0	0	0	0
0.2	$4.9642766368 \times 10^{-6}$	$4.9623818179 \times 10^{-6}$	$4.9621910116 \times 10^{-6}$	$4.9621892665 \times 10^{-6}$	$4.9621906865 \times 10^{-6}$
0.4	$2.4995308230 \times 10^{-5}$	$2.4991894407 \times 10^{-5}$	$2.4992127719 \times 10^{-5}$	$2.4992110504 \times 10^{-5}$	$2.4992113393 \times 10^{-5}$
0.6	$1.1983184636 \times 10^{-4}$	$1.1982841990 \times 10^{-4}$	$1.1982829315 \times 10^{-4}$	$1.1982830889 \times 10^{-4}$	$1.1982831266 \times 10^{-4}$
0.8	$4.9549557561 \times 10^{-4}$	$4.9549378243 \times 10^{-4}$	$4.9549365732 \times 10^{-4}$	$4.9549364391 \times 10^{-4}$	$4.9549363996 \times 10^{-4}$
1	$1.3552461378 \times 10^{-3}$	$1.3552449765 \times 10^{-3}$	$1.3552452541 \times 10^{-3}$	$1.3552451641 \times 10^{-3}$	$1.3552451986 \times 10^{-3}$

TABLE 13. The values of $V(x)$ for $\sigma = 0.5$, $k = 0$ and different values of N .

x	$N = 20$	$N = 25$	$N = 30$	$N = 35$	$N = 40$
0	0.1	0.1	0.1	0.1	0.1
0.2	0.0408380754	0.0408380099	0.0408380010	0.0408380034	0.0408380057
0.4	0.0318824589	0.0318824680	0.0318824702	0.0318824677	0.0318824694
0.6	0.0272018958	0.0272019248	0.0272019106	0.0272019096	0.0272019118
0.8	0.0243554452	0.0243554697	0.0243554752	0.0243554764	0.0243554768
1	0.0227352531	0.0227353251	0.0227353051	0.0227353118	0.0227353091



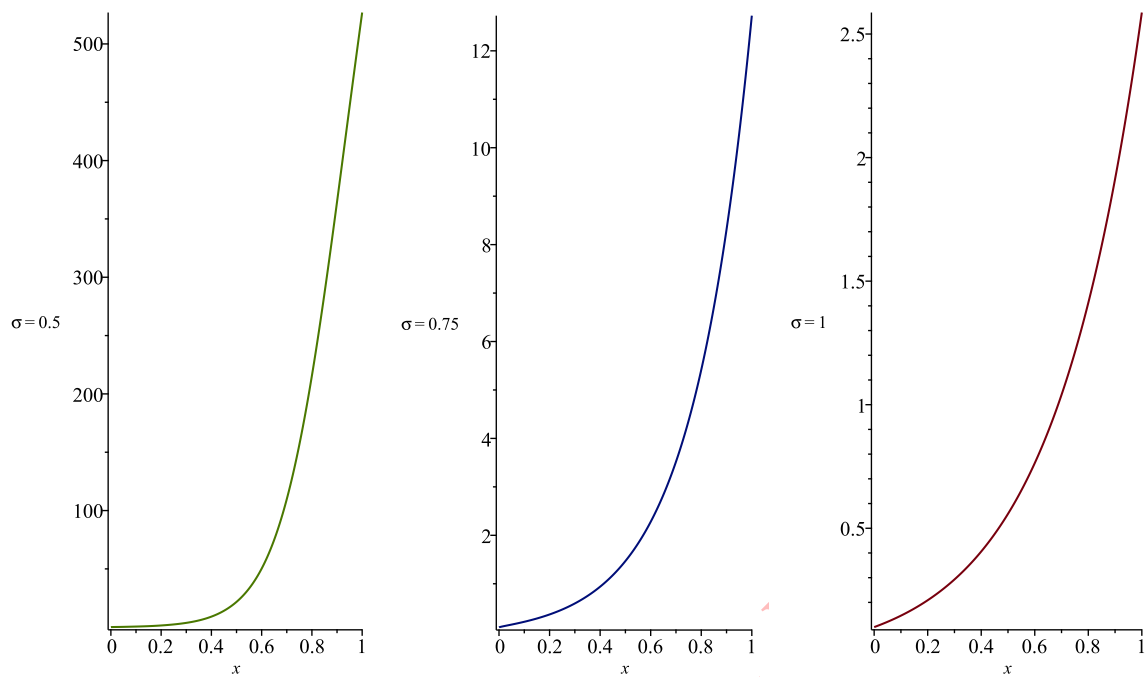


FIGURE 1. Graph of $T(x)$ using the presented method for $N = 20$, $k = 0$ and different values of σ .

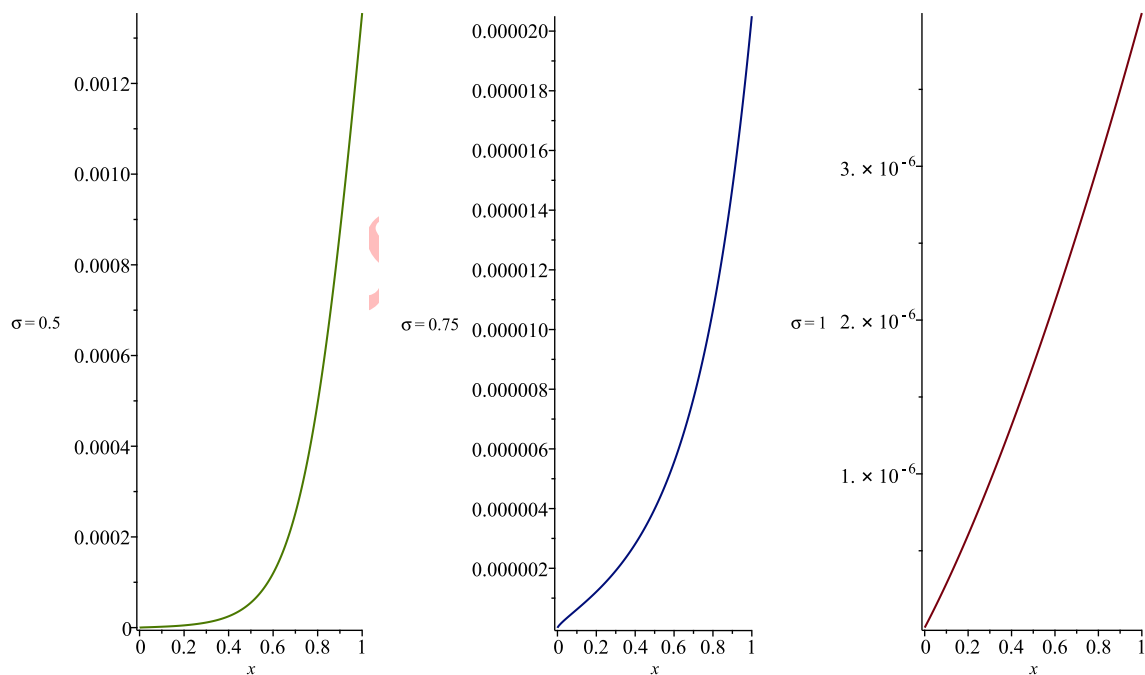


FIGURE 2. Graph of $I(x)$ using the presented method for $N = 20$, $k = 0$ and different values of σ .



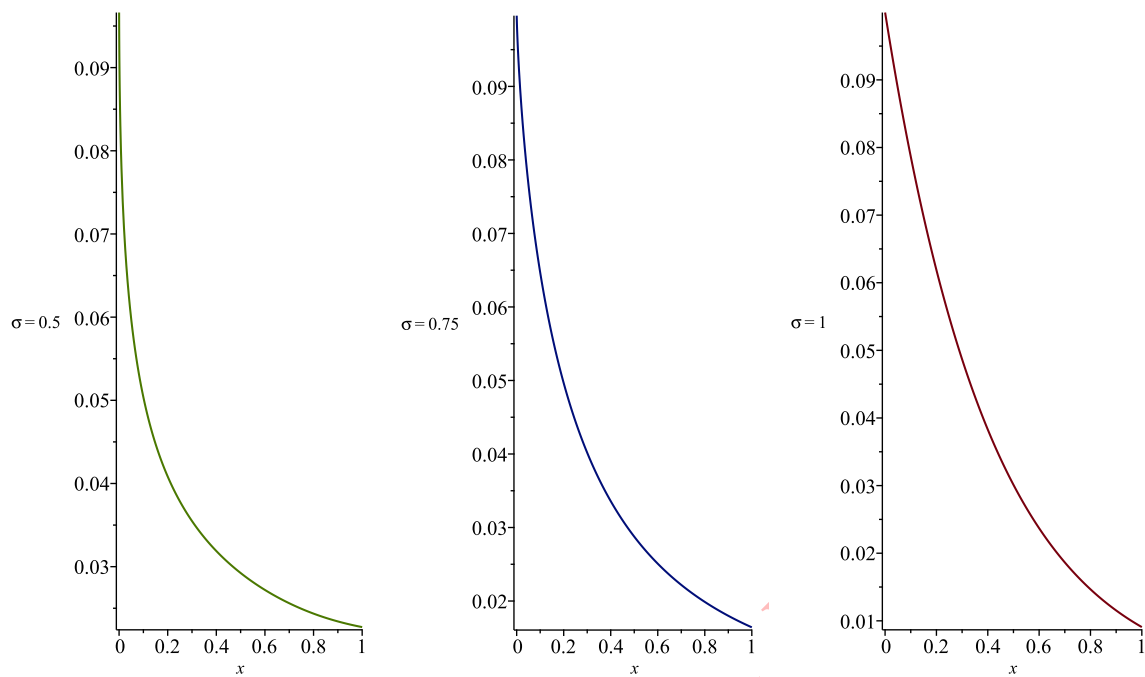


FIGURE 3. Graph of $V(x)$ using the presented method for $N = 20$, $k = 0$ and different values of σ .

Uncorrected

REFERENCES

- [1] M. Aghashahi and M. R. Gandomani, *Numerical solution of Fractional Differential Equation system using the Müntz-Legendre Polynomials*, Int. J. Pure Appl. Math., 115(3) (2017), 467–475.
- [2] S. Akhlaghi, M. Tavassoli Kajani, and M. Allame, *Numerical Solution of Fractional Order Integro-Differential Equations via Müntz Orthogonal Functions*, J. Math., 2023 (2023), 6647128, 1–13.
- [3] S. Akhlaghi, M. Tavassoli Kajani, and M. Allame, *Application of Müntz Orthogonal Functions on the Solution of the Fractional Bagley-Torvik Equation Using Collocation Method with Error Estimate*, Adv. Math. Phys., 2023 (2023), 5520787, 1–11.
- [4] R. Amin, S. Yuzbasi, and S. Nazir, *Efficient Numerical Scheme for the Solution of HIV Infection CD_4^+ T-Cells Using Haar Wavelet Technique*, CMES-Comput. Model. Eng. Sci., 130(3) (2022), 639–653.
- [5] H. D. Azodi and M. R. Yaghouti, *A new method based on fourth kind Chebyshev wavelets to a fractional order model of HIV infection of CD_4^+ T cells*, Comput. Meth. Differ. Equ., 6(3) (2018), 353–371.
- [6] A. Babaei, H. Jafari, and S. Banihashemi, *Numerical solution of variable order fractional non-linear quadratic integro-differential equations based on the sixth-kind Chebyshev collocation method*, J. Comput. Appl. Math., 377 (2020), 112908.
- [7] D. Baleanu, K. Diethelm, E. Scalas, and J. J. Trujillo, *Fractional calculus*, in: *Series on Complexity, Nonlinearity and Chaos*, Vol. 3, World Scientific Publishing Co. Pvt. Ltd., Hackensack, NJ, 2012.
- [8] C. Canuto, M. Y. Hussaini, A. Quarteroni, and T. A. Zang, *Spectral Methods. Fundamentals in Single Domains*, Springer, Berlin Heidelberg New York, 2006.
- [9] B. Celik, A. O. Akdemir, E. Set, and S. Aslan, *Ostrowski-Mercer Type Integral Inequalities For Differentiable Convex Functions Via Atangana-Baleanu Fractional Integral Operators*, TWMS J. Pure Appl. Math., 15(2) (2024), 269–285.
- [10] S. Erman, A. Demir, and E. Ozbilge, *Solving inverse non-linear fractional differential equations by generalized Chelyshkov wavelets*, Alexandria Eng. J., 66 (2023), 947–956.
- [11] N. R. Gande and H. Madduri, *Higher order numerical schemes for the solution of fractional delay differential equations*, J. Comput. Appl. Math., 402 (2022), 113810.
- [12] M. R. Gandomani and M. T. Kajani, *Numerical Solution of a Fractional Order Model of HIV Infection of CD_4^+ T Cells Using Müntz-Legendre Polynomials*, Int. J. Bioautomation, 20(2) (2016), 193–204.
- [13] M. R. Gandomani and M. Tavassoli Kajani, *Application of shifted Müntz-Legendre Polynomials for solving fractional differential equations*, Int. J. Pure Appl. Math., 103(2) (2015), 263–279.
- [14] P. Goel, D. Singh, D. Gopal, and H. Aydi, *F-Kannan Mappings In Non-Triangular Metric Spaces And Applications To Integral And Fractional Calculus*, TWMS J. Pure Appl. Math., 16(1) (2025), 19–43.
- [15] E. Gokmen, B. Gurbuz, and M. Sezer, *A numerical technique for solving functional integro-differential equations having variable bounds*, Comput. Appl. Math., 37 (2018), 5609–5623.
- [16] S. Irandoust-pakchin, S. Abdi-mazraeh, and H. Kheiri, *Construction of new generating function based on linear barycentric rational interpolation for numerical solution of fractional differential equations*, J. Comput. Appl. Math., 375 (2020), 112799.
- [17] D. Jain, A. Bhargava, and S. Gupta, *A New Approach to Population Growth Model Involving a Logistic Differential Equation of Fractional Order*, Crit. Rev. Biomed. Eng., 53(2) (2025), 37–48.
- [18] R. Katani, S. Shahmorad, and D. Conte, *Approximate solution of multi-term fractional differential equations via a block-by-block method*, J. Comput. Appl. Math., 453 (2025), 116135.
- [19] J. Li, X. Su, and K. Zhao, *Barycentric interpolation collocation algorithm to solve fractional differential equations*, Math. Comput. Simul., 205 (2023), 340–367.
- [20] M. R. Lemnaouar and K. Hattaf, *On a class of fractal-fractional differential equations with generalized fractal derivatives and non-singular kernels: a theoretical and numerical study*, Nonlinear Dyn., 113 (2025), 13061–13079.
- [21] X. Liu and M. Jia, *A class of iterative functional fractional differential equation on infinite interval*, Appl. Math. Lett., 136 (2023), 108473.
- [22] M. Maleki and M. Tavassoli Kajani, *Numerical approximations for Volterra’s population growth model with fractional order via a multi-domain pseudospectral method*, Appl. Math. Model., 39 (2015), 4300–4308.



- [23] H. R. Marzban, *A generalization of Müntz-Legendre polynomials and its implementation in optimal control of non-linear fractional delay systems*, *Chaos Solitons Fractals*, 158 (2022), 112093.
- [24] M. Merdan, A. Gokdogan, and A. Yildirim, *On the Numerical Solution of the Model for HIV Infection of CD₄+T Cells*, *Comput. Math. Appl.*, 62(1) (2011), 118–123.
- [25] G. V. Milovanović, *Müntz orthogonal polynomials and their numerical evaluation*, *Applications and Computation of Orthogonal Polynomials*, Springer, Oberwolfach Germany, 1998, 179–194.
- [26] M. Y. Ongun, *The Laplace Adomian Decomposition Method for Solving a Model for HIV Infection of CD₄+T Cells*, *Math. Comput. Model.*, 53(6) (2011), 597–603.
- [27] O. Postavaru and A. Toma, *Numerical solution of two-dimensional fractional-order partial differential equations using hybrid functions*, *Partial Differ. Equ. Appl. Math.*, 4 (2021), 100099.
- [28] M. Pourbabaee and A. Saadatmandi, *A new operational matrix based on Müntz-Legendre polynomials for solving distributed order fractional differential equations*, *Math. Comput. Simul.*, 194 (2022), 210–235.
- [29] A. Roohollahi, B. Ghazanfari, and S. Akhavan, *Numerical solution of the mixed Volterra-Fredholm integro-differential multi-term equations of fractional order*, *J. Comput. Appl. Math.*, 376 (2020), 112828.
- [30] L. Sadek, S. Yuzbasi, and H. T. Alaoui, *Two numerical solutions for solving linear and nonlinear systems of differential equations*, *Appl. Comput. Math. Int. J.*, 23(4) (2024), 421–436.
- [31] M. Saffarian and A. Mohebbi, *Numerical solution of two and three dimensional time fractional damped non-linear Klein-Gordon equation using ADI spectral element method*, *Appl. Math. Comput.*, 405 (2021), 126182.
- [32] D. Shirani, M. Tavassoli Kajani, and S. Salahshour, *Numerical Solution of a SIR Fractional Model of the Distribution of Computer Viruses Using Dickson Polynomials*, *Int. J. Ind. Math.*, 13(3) (2021), 323–331.
- [33] M. Tavassoli Kajani, *Numerical solution of fractional pantograph equations via Müntz-Legendre polynomials*, *Math. Sci.*, 18 (2024), 387–395.
- [34] S. N. Tural-Polat and A. T. Dincel, *Numerical solution method for multi-term variable order fractional differential equations by shifted Chebyshev polynomials of the third kind*, *Alexandria Eng. J.*, 61(7) (2022), 5145–5153.
- [35] Vivek, M. Kumar, and S. N. Mishra, *A fast Fibonacci wavelet-based numerical algorithm for the solution of HIV-infected CD₄⁺T cells model*, *Eur. Phys. J. Plus*, 138(5) (2023), 458.
- [36] H. Y. Xu, M. M. Khalsaraei, A. Shokri, H. Ramos, and M. Molayi, *Nonstandard finite difference schemes with positivity property with application to a mathematical model of HIV infection*, *Appl. Comput. Math. Int. J.*, 23(4) (2024), 541–557.
- [37] C. Yang, *Improved spectral deferred correction methods for fractional differential equations*, *Chaos Solitons Fractals*, 168 (2023), 113204.
- [38] X. Ye, J. Cao, and C. Xu, *A High Order Scheme for Fractional Differential Equations with the Caputo-Hadamard Derivative*, *J. Comput. Math.*, 43(3) (2025), 615–640.
- [39] S. Yuzbasi, *A numerical approach to solve the model for HIV infection of CD₄+T cells*, *Appl. Math. Model.*, 36(12) (2012), 5876–5890.

